Experimental study on a three-dimensional passive earth pressure coefficient in cohesionless soil

P. Capilleri[1], E. Motta[2]*, M. Todaro[2] and G. Biondi[3]

[1] Department of Civil and Industrial Engineering, University of Pisa,
Largo Lucio Lazzarino, 81031, Pisa, (Italy)
[2] Department of Engineering and Architecture, University of Catania,
Via Santa Sofia 64 Catania, (Italy)
*emotta@dica.unict.it

[3] Department of Engineering, University of Messina,
Contrada di Dio (S. Agata) - 98166 Messina, (Italy)

Abstract. Estimation of the passive earth pressure is a crucial aspect in several geotechnical design problems. Several authors presented two-dimensional models for its evaluation while three-dimensional (3D) approaches have received less attention. It has been recognized that in many geotechnical systems, such as anchor blocks or plates or everywhere the width of the load area is limited if compared to its height, the three-dimensional passive earth pressure is quite different from the two-dimensional one and, due to side effects, is generally larger. This paper is concerned with an experimental and numerical study of 3D passive earth pressure encountered by a rigid plate of limited width in a cohesionless soil. The obtained results allowed the evaluation of a three-dimensional passive earth pressure coefficient which is not only dependent on the soil friction angle, as it occurs in a 2D formulation, but also on the ratio of the width to the height of the load area.

Keywords: passive earth pressure, model test, numerical analysis, cohesionless soil, three-dimensional analysis.

1 Introduction

The magnitude of the passive earth pressure is controlled by several factors such as strength and stiffness of the soil, friction or adhesion at the interface between the structure and soil, shape of the structure and displacement level. The evaluation of the limit passive earth pressure is of significant practical importance and dealing with the design of diaphragm walls, anchors and foundations. Most of the available researches aim to refine the Coulomb and Rankine two-dimensional approaches under static or seismic loading conditions. Solutions based on limit-equilibrium (Kapila 1962; Shields and Tolunay 1973; Rahardjo and Fredlund 1984; Zakerzadeh et al. 1999, Subba Rao and

Choudhury, 2005), slip line (Caquot and Kerisel 1949; Sokolovski 1960) or limit analyses (Lysmer 1970; Lee and Herington 1972; Soubra 2000; Lancellotta 2002, 2007) approaches have been presented in literature. Most of available solutions concern with two-dimensional approaches for plane-strain conditions. Several geotechnical systems, such as anchor blocks or plates, diaphragm walls of a limited width and laterally loaded pile caps, mobilize the passive earth pressure in a three-dimensional manner. However, the problem of 3D passive earth pressure evaluation has received less attention, and this is indeed due also to the difficulties inherently involved in the study of a 3D failure mechanism and in proposing proper analytical solutions. Blum (1932) and Soubra and Regenass (2000) proposed 3D solutions based on the limit equilibrium and the upper bound theorem of the limit analysis, respectively. 3D numerical analyses, based on finite difference method, were presented by Benmebarek et al. (2008) and Benmeddour et al. (2010) even if closed form solutions were not provided. None of these analyses take into account the seismic effects and/or the slope inclination, so they cannot be applied in several cases concerned with geotechnical design in seismic areas. Recently Motta and Raciti (2014) presented an extension of the classical Mononobe-Okabe-Kapila method and provided a limit equilibrium closed form solution for the evaluation of a 3D passive earth pressure coefficient accounting for the soil-wall interface friction angle, for the slope of the soil mass involved in the plastic mechanism and for the seismic effects accounted for through a pseudo-static approach.
In this paper the experimental results concerned with 3D passive earth pressure are presented together with the main features of the physical model adopted in the tests. The obtained results were compared with the results of a set of FEM numerical analyses and allowed the evaluation of a 3D passive earth pressure coefficient which depends on the soil friction angle and on the ratio of the width to the height of the loading area.

2 Experimental physical modelling

Soil mechanical properties influence the magnitude of the passive earth pressure and its mobilization with soil displacements. A first set of experiments were conducted by Terzaghi (1920) that assembled an experimental setup using a box containing dry sand and a 0.05 m high wall on one side of the box. His observations underlined that the passive earth resistance depends on the magnitude of the wall displacements and on the soil mechanical properties with particular reference to the soil relative density.

5.1 Model set-up

The physical model adopted in this study is shown in Figures 1 and 2 and consisted in a wooden box (87 x 70 x 40 cm), containing sand, integrated with a hydraulic piston acting on a steel plate and connected to an oil pump and to a data acquisition system. Instru-

ments include also a displacement transducer and a pressure cell. The oil pump connected to the hydraulic piston was capable of working at a maximum pressure of 700 Bar. The transducer was connected to the piston by a magnetic fixing system, reading the displacements of the rigid load plate in contact with the sand and able to induce a passive pressure. To measure the load applied to the plate during the test, the load cell was installed between the piston and the steel plate.

The wooden box was filled with a uniform silica sand, called Catania "Plaja sand", that was previously characterized from a static and a dynamic point of view (Capilleri et al, 2019, Cavallaro et., 2018, Banna et al, 2015, Capilleri et al., 2014). For this sand the specific gravity is G_s = 2.65, the maximum and minimum dry unit weight are $\gamma_{d,max}$ = 16.5 kN/m^3 and $\gamma_{d,min}$ = 14.2 kN/m^3, respectively and the uniformity coefficient is C_U = 2.

In all the tests the height of the sand strata in contact with the steel plate is H = 15 cm (Fig. 2a). The local control of the soil relative density was obtained through the pluvial deposition technique (Fig. 3a), with a constant fall height for each deposited sand layer. In the experiment, the selected height of deposition allowed to obtain a sand relative density D_r of about 60 % leading to a soil unit weight of about γ = 15.5 kN/m^3 and to a friction angle equal to ϕ' = 38°, as estimated by direct shear test results.

Once the sand was settled into the wooden box, red colored pins were regularly positioned at the soil free surface (Fig. 3b) to better visualize the soil mass movement and the passive failure process during the test.

Actuating the hydraulic pump and making the plate moving forward against the soil, the sand deposit brought to a passive failure condition. The rigid plates utilized to induce the passive earth pressure on the sand were characterized by different ratios B/H, B and H = 15 cm being the width and the height of the plate in contact with the sand.

On the whole, 10 tests were carried out using plates having B/H equal to 0.5, 1 and 2. The experiments included also a series of preliminary calibration tests.

The data collected during the tests have been processed and collected and are summarized in Figure 4 in the form of load–displacement curves.

At the end of each test, the dimensions of the passive soil wedge involved in the failure mechanism were also detected at the soil free surface. As shown in Figure 5, in all the tests the same value of the maximum wedge dimension in the direction orthogonal to the loading plate were observed, with an average value of about 30 cm which is twice the height H of the loading area. From the experimental measurements of the passive earth pressure load S_P, a passive earth pressure coefficient k_P was determined:

$$k_p = \frac{2 \cdot S_p}{\gamma \cdot H^2 \cdot B} \quad (1)$$

3 Numerical modelling

A 3D numerical analysis aimed to reproduce the experimental results was also carried out using the computer code ADINA. The ADINA code uses an explicit finite element program to study numerically the mechanical behavior of a continuous 3D medium as

it reaches equilibrium or steady plastic flow. The explicit Lagrangian calculation scheme and the mixed-discretization zoning technique ensure that plastic failure and flow are modelled very accurately.

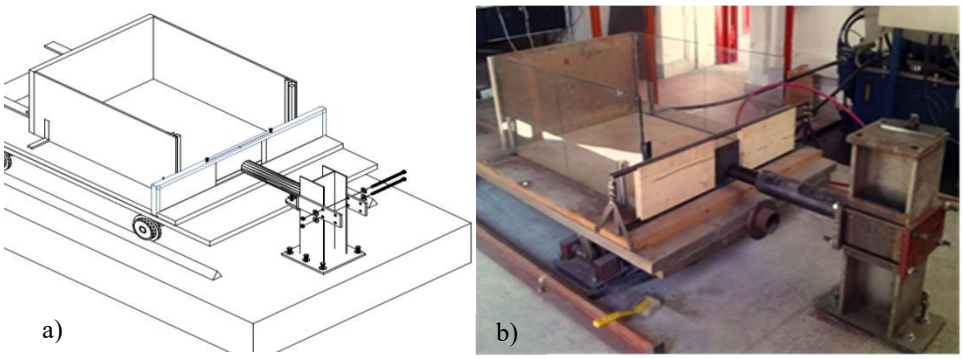

Fig. 1 Experimental facility: (a) axonometric view; (b) photo.

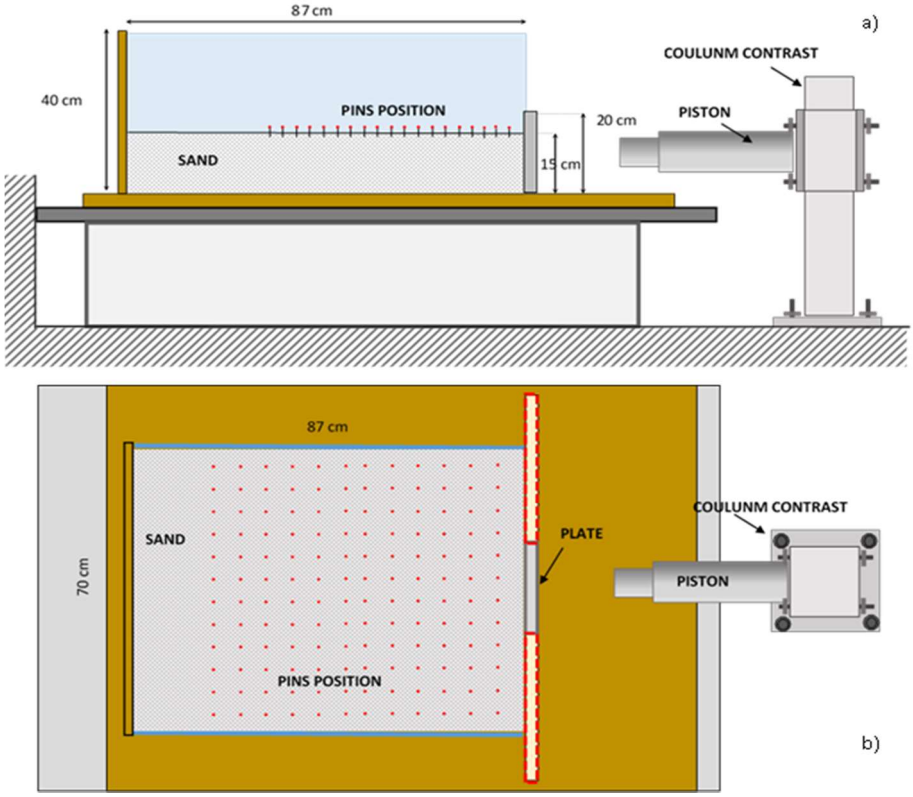

Fig. 2 Schematic of the experimental setup: (a) section view; (b) plan view

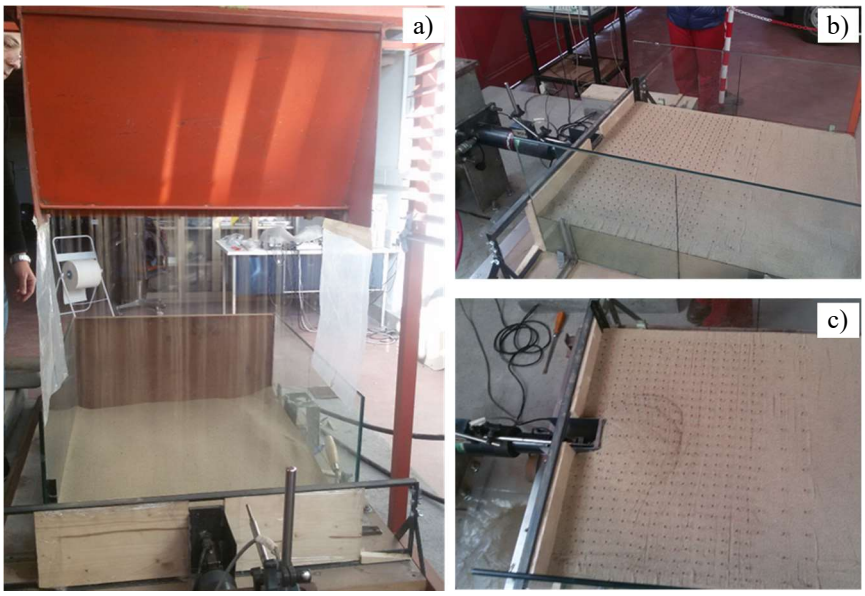

Fig. 3 Model set-up: (a) sand pluvial deposition; configuration of the physical model before (b) and after (c) the test.

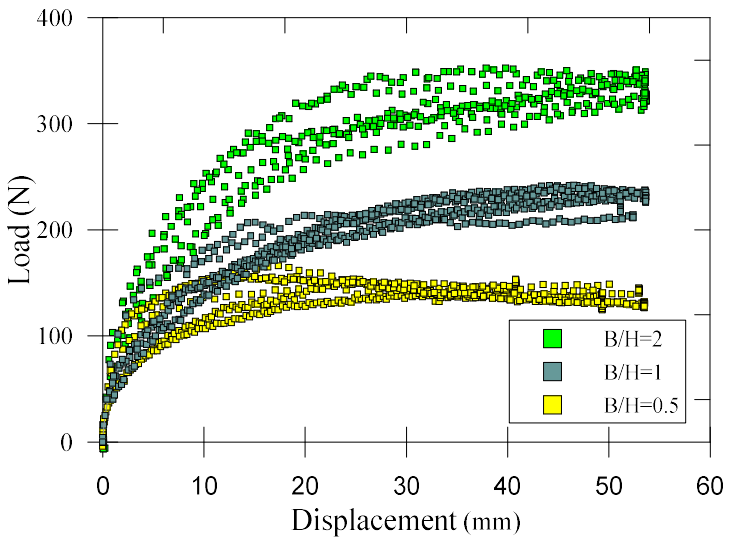

Fig. 4 Load-displacement curves obtained for three different value of the width *B* to height *H* ratio of the loading area.

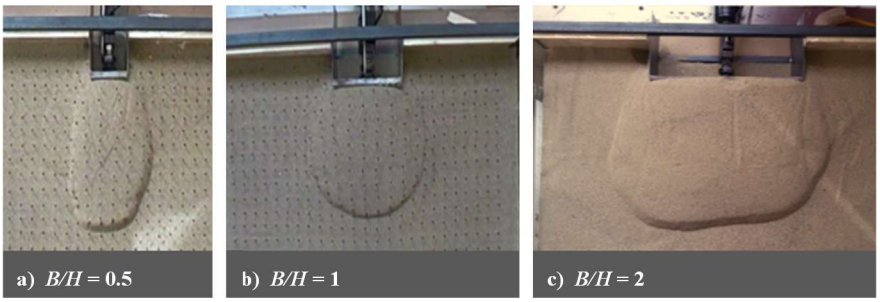

Fig. 5 Geometry of the passive soil wedge detected at the end of the tests at the soil free surface: a) $B/H = 0.5$; b) $B/H = 1$; c) $B/H = 2$

The numerical model adopted in the analyses consists in a soil volume and a steel plate having the same dimensions of the actual physical model. The effects of the hydraulic piston acting on the steel plate was simulated through a concentrated horizontal force applied to the plate at one third of its height from the bottom of the soil model.

Figure 6 shows the numerical models adopted in the analyses which were carried out for values of the width to height ratio B/H ranging from 0.1 to 3. Specifically, the numerical results obtained for the cases $B/H = 0.5$, 1.0 and 2.0 were used for a systematic comparison with the experimental measurements; as described later in the paper, the results of the other numerical analyses (carried out for B/H ratios equal to 0.1, 0.25, and 3), were adopted to confirm the general trends the experimental and numerical results.

In the FEM analyses the soil was modeled as an elastic-perfectly plastic material obeying to the Mohr-Coulomb failure criterion. An associate flow-rule was considered together with a Young modulus $E = 4$ MPa, a Poisson ratio $\nu = 0.35$, a soil unit weight $\gamma = 15.5$ kN/m^3 and friction angle equal to $\phi' = 38°$. For the steel plate an elastic soil behavior was assumed with a very high Young modulus to simulate a rigid behavior. Due to the smoothness of the steel plate surfaces, the sand-plate interface has been assumed as a smooth surface in the analyses.

The ultimate passive limit state in the numerical model was obtained by increasing the force acting against the plate, until an abrupt increment in the horizontal displacement of the plate was attained, implying that the passive failure condition is attained.

The corresponding force applied to the plate was assumed as the numerical value of the 3D passive limit load S_P. The deformed mesh and the displacement contours provided by the FEM analyses once the failure condition is reached are shown in Figure 7 while the values of S_P are plotted in Figure 8a versus the width to height ratio B/H.

Starting from the numerical estimates of S_P, the values of the 3D passive earth pressure coefficient k_P were also estimated according to eq. (1) and are plotted inf Figure 8b.

In Figure 8, consistently with the assumption of a smooth surface at the sand-plate interface ($\delta = 0$), also the values of S_P and k_P obtained using the 2D and 3D passive earth pressure coefficients provided by the Rankine theory and by Motta and Raciti (2014), respectively, are plotted for comparison. The values of a passive earth pressure coefficient k_P were determined from the passive earth pressure load at failure, S_P, utilizing equation 1.

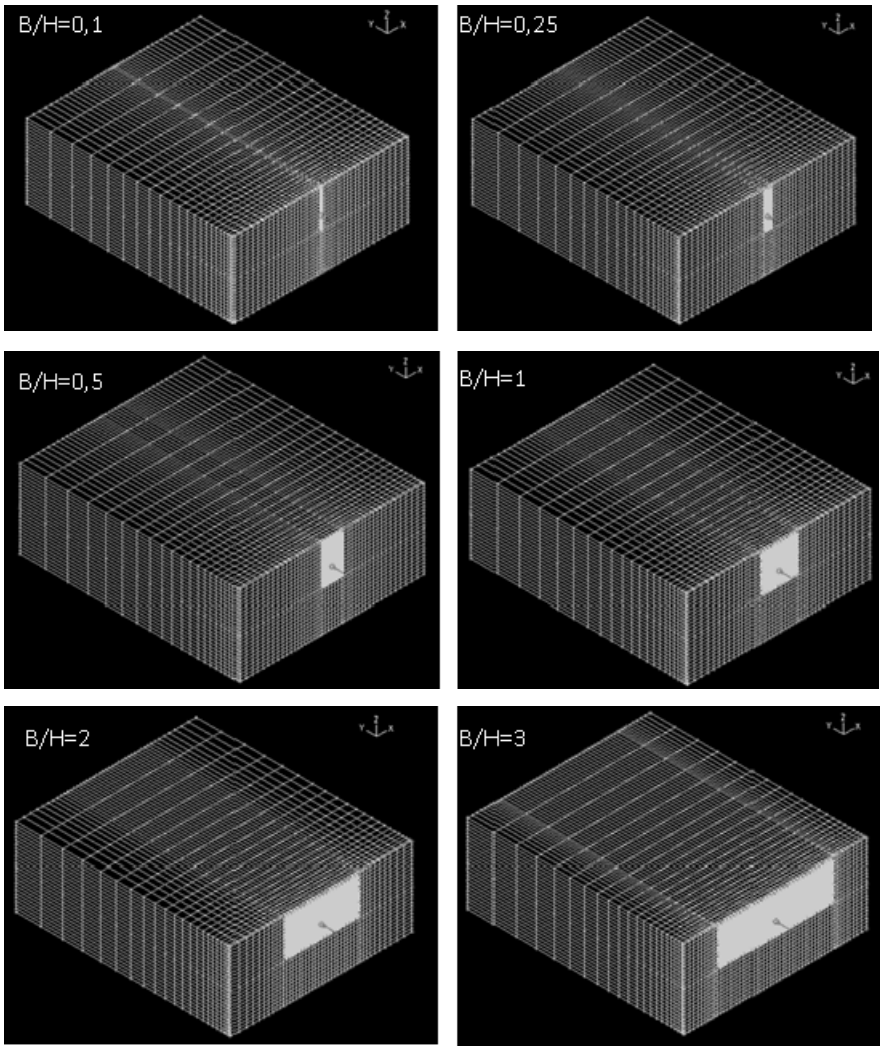

Fig. 6 FEM models adopted in the FEM analyses carried out for different loading plate dimensions.

A general fair agreement between experimental data, FEM analysis results and prediction obtained with the Motta and Raciti (2014) solution can be observed in terms of both S_P (Fig. 8a) and k_P (Fig. 8b). Obviously, the passive failure load given by the Rankine theory increases linearly with the width B, being k_P the same regardless of B/H ratios. Regardless B/H, the theoretical values of the 2D passive earth-pressure coefficient deduced from the Rankine theory are lower than the corresponding 3D experimental values with differences that reduce as the ratio B/H increases approaching a plain strain conditions.

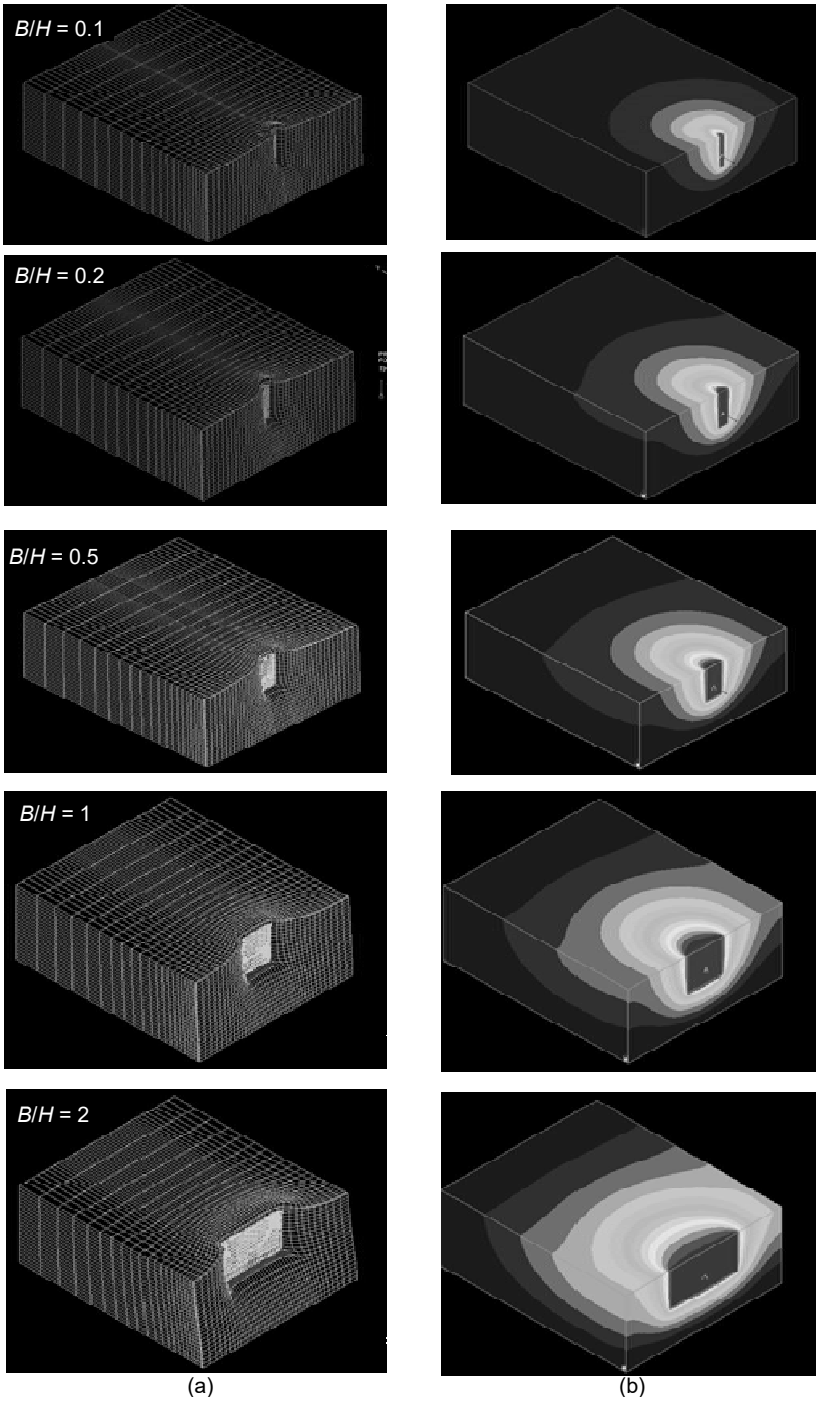

Fig. 7 FEM analysis results: deformed mesh (column a) and displacements contours (column b).

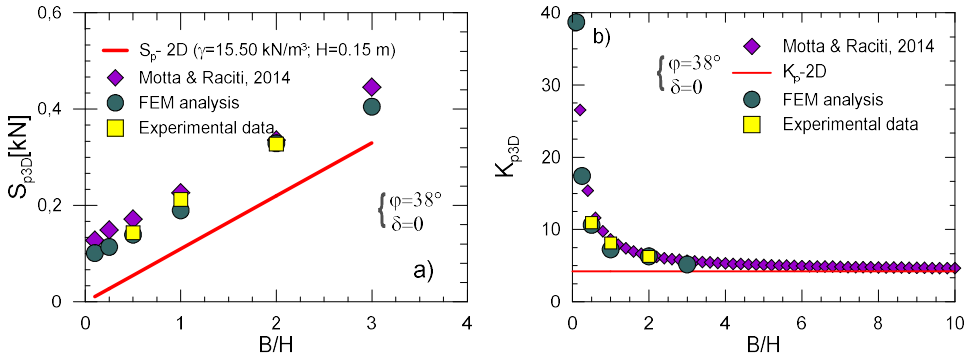

Fig. 8 Comparison between FEM analysis results, experimental data and numerical prediction obtained using the solution by Motta & Raciti (2014): (a) earth pressure values; (b) earth pressure coefficient**.**

5 Conclusions

Values of a 3D earth pressure coefficient have been determined from a series of experimental tests and from numerical FEM analysis results. Loading plates with width to height ratio *B*/*H* in the range 0.5-2 have been adopted in the tests to induce the passive failure conditions in a uniform silica sand deposit obtained through the pluvial deposition technique. The results of the FEM simulations, carried out for *B*/*H* in the range 0.1-0.3, are in a fair agreement with the experimental data and highlighted that the 3D passive earth pressure coefficient k_P is much higher than that provided by the 2D Rankine theory. Experimental 3D values of k_P are also in a good agreement with the 3D limit equilibrium theoretical solution proposed by Motta e Raciti (2014). Finally, the experimental results indicate that the 3D passive limit load for lower values of ratio *B*/*H* are significantly greater than the 2D values and the 3D passive earth pressure coefficient k_P reduces in a strongly nonlinear way with *B*/*H* ratio. For large values of *B*/*H*, the differences between 3D and 2D values of k_P reduce since the system approaches a plain strain condition and the side resistance of the 3D failure mechanism become negligible.

References

ADINA, Automatic Dynamic Incremental Nonlinear Analysis. Theory and modelling guide, Adina R&D, Inc. Watertown, USA 2008.

Banna, G., Capilleri, P., Massimino, M.R., Motta, E. (2015). Geotechnical characterization of Mount Etna ash for its reuse preserving human health. Volcanic Rocks and Soils – Proc. International Workshop on Volcanic Rocks and Soils, 2015: 127-128.

Benmebarek S., T. Khelifa, N. Benmebarek, R. Kastner (2008). Numerical evaluation of 3D passive earth pressure coefficients for retaining wall subjected to translation. Computers and Geotechnics 35, 47–60.

Benmeddour D., Mellas M., Mabrouki A. (2010). Etude Numerique Des Pressions Passives Appliquees Sur Un Bloc D'ancrage Rigide. Courrier du Savoir N°10, Avril 2010,43-49.

Blum H. (1932). Wirtschaftliche Dalbenformen und deren Berechnung. Bautechnik, 10(5), 122–135 (in German).

Capilleri P., Cavallaro A.,Motta e., Todaro M. (2019). Dynamic characterization of sands used as backfill in a reinforced earth wall. 7th International Conference on Earthquake Geotechnical Engineering 17 - 20 June 2019 • Roma. Paper N 10250. (accepted for publication)

Capilleri, P. P., Cavallaro, A., Maugeri, M. (2014). Static and dynamic soil characterization at Roio piano (AQ). Rivista Italiana di Geotecnica, 48(2), 38-52.

Cavallaro, A., Capilleri, P., & Grasso, S. (2018). Site Characterization by Dynamic In Situ and Laboratory Tests for Liquefaction Potential Evaluation during Emilia Romagna Earthquake. Geosciences, 8(7), 242.

Caquot A., Kerisel J. (1949). Traite de mecanique des sols. Gauthier-Villars, Paris (in French).

Kapila, J. P. (1962). Earthquake Resistant Design of Retaining Walls. 2nd Earthquake Symposium, University of Roorkee, Roorkee, India.

Lancellotta R. (2002). Analytical solution of passive earth pressure, Geotechnique, Vol. 52, No. 8, 617-619.

Lancellotta R. (2007). Lower-Bound approach for seismic passive earth resistance. Geotechnique, Vol. 57, No. 3, 319-321.

Lee I. K., Herington J. R. (1972). A theoretical study of the pressures acting on a rigid wall by a sloping earth on rockfill. - Geotechnique, London, 22(1), 1–26.

Lysmer J. (1970). Limit analysis of plane problems in soil mechanics. Journal for Soil Mechanics and Foundation Division, ASCE, 96, No. 4, 1311-1334.

Motta E., Raciti E. (2014). A closed form solution for a three dimensional passive earth pressure coefficient. Italian Geotechnical Journal, No.3, pp. 7-17.

Rahardjo, H., And Fredlund, D. G. (1984). General limit equilibrium method for lateral earth force. Canadian Geotechnical Journal, Ottawa, 21(1), 166–175.

Shields, D. H., Tolunay, A. Z. (1973). Passive pressure coefficients by methods of slices. Journal of Soil Mechanics and Foundation Division, ASCE, 99(12), 1043–1053.

Sokolovski, V. V. (1960). Static of soil media. Butterworth's scientific publications, London, 237 pp.

Soubra A.-H. (2000). Static and seismic passive earth pressure coefficients on rigid retaining structures. Canadian Geotechnical Journal, 2000, 37(2), 463-478.

Terzaghi K. (1920). Soil mechanics in engineering practice. John Wiley & Sons Inc., New York.

Soubra A.H., Regenass, P. (2000). Threedimensional passive earth pressures by kinematical approach. Journal of Geotechnical and Geoenvironmental Engineering, ASCE, 2, No.2, 969-978.

Subba Rao, K. S. And Choudhury, D. (2005). Seismic passive earth pressures in soils. Journal of Geotechnical and Geoenvironmental Engineering, ASCE, 131(1), 131-135.

Zakerzadeh, N., Fredlund, D. G., Pufahl, D. E. (1999). Interslice force functions for computing active and passive earth force. Canadian Geotechnical Journal, Ottawa, 36(6), 1015–1029.